Available online at www.sciencedirect.com
ScienceDirect
Journal of Sound and Vibration 305 (2007) 918–924
JOURNAL OF SOUND AND VIBRATION
www.elsevier.com/locate/jsvi

Short Communication

Wave propagation in a constrained fluid layer bounded by an elastic half-space and its relevance in cochlear micromechanics

Stephen J. Elliott

Institute of Sound and Vibration Research, University of Southampton, Southampton, UK

Received 5 December 2006; received in revised form 23 April 2007; accepted 23 April 2007
Available online 7 June 2007

Abstract

Wave propagation is investigated in a thin fluid layer bound by a rigid surface and an elastic half-space. Slow waves are possible if the fluid gap is small compared with the wavelength of the Rayleigh wave in the elastic half-space. The relevance of such a wave in cochlear micromechanics is discussed, which leads to the incorporation of the fluid viscosity and elastic loss into the wave equation. For typical parameters in the cochlea, the wave is dominated by the stiffness of the elastic half-space and the viscosity of the fluid, decaying significantly within a wavelength.

1. Introduction

Various types of waves can propagate in fluid-elastic systems. Constrained fluid layers bounded by thin plates have been considered by Lloyd and Redwood [1,2] and have been shown to support a type of squirting wave, in which the inertia of the constrained fluid layer interacts with the bending stiffness of the plate. In this paper, we consider waves that may propagate in a constrained fluid layer bounded by an elastic half-space. The existence of slow waves under these conditions was predicted by Krauklis et al. [3], in the context of wave propagation in an oil-filled layer between two geological strata.

Our motivation for investigating this geometry came from the possibility of wave propagation in the thin fluid layer between the tectorial membrane and reticular lamina in the cochlea. For the dimensions within the cochlea, viscous losses within the fluid are shown to be important, both in significantly reducing the propagation speed, as well as in attenuating the wave.

2. Fluid-elastic waves

Consider the equation governing waves in a fluid layer of thickness d bounded by an elastic half-space and a rigid surface, so that the fluid layer is constrained as shown in Fig. 1. All the variables are considered constant in the y direction so that only waves which propagate along the x direction are considered. The analysis would

E-mail address: sje@isvr.soton.ac.uk

0022-460X/$ - see front matter
doi:10.1016/j.jsv.2007.04.040

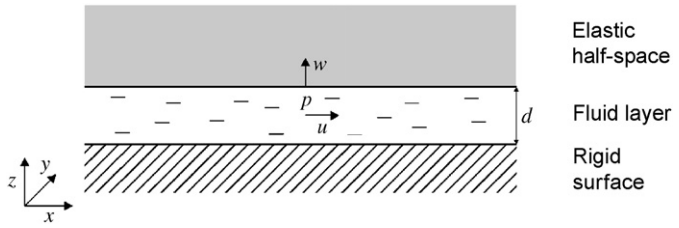

Fig. 1. The modelled geometry of the constrained fluid layer, in which the longitudinal fluid displacement is u and the pressure is p, between a rigid surface and an elastic layer on which the transverse surface displacement is w.

be the same if a fluid layer of twice the thickness was bounded by two identical elastic half-spaces which moved symmetrically.

Starting off in the time domain, we define the transverse wall displacement at the surface of the elastic layer, in the z direction, as being w, the fluid displacement, in the x direction, as being u and the fluid pressure to be p, which are all functions only of x and t. The fluid in the gap is assumed to be incompressible, so that conservation of mass for an elemental slice in the gap leads to a relationship between the transverse wall displacement and radial fluid flow

$$\frac{\partial u}{\partial x} = -\frac{w}{d}. \tag{1}$$

Ignoring the effect of fluid viscosity for the time being, the conservation of fluid momentum leads to the equation

$$\frac{\partial p}{\partial x} = -\rho \frac{\partial^2 u}{\partial t^2}, \tag{2}$$

where ρ is the fluid density. Differentiating Eq. (1) twice with respect to t and comparing this with Eq. (2) differentiated with respect to x then gives

$$\frac{\partial^2 p}{\partial x^2} - \frac{\rho}{d}\frac{\partial^2 w}{\partial t^2} = 0. \tag{3}$$

The pressure and wall displacements are now assumed to be equal to $p(\omega, k)e^{j(\omega t - kx)}$ and $w(\omega, k)e^{j(\omega t - kx)}$, respectively, where ω is the angular frequency and k is the wavenumber, so that Eq. (3) can be written as

$$-k^2 p(\omega, k) + \frac{\omega^2 \rho}{d} w(\omega, k) = 0. \tag{4}$$

The ratio of $p(\omega, k)$ to $w(\omega, k)$, which can be termed the wall stiffness, has been analysed for an elastic half-space by Graff [4], for example, who shows that it can be written as

$$\frac{p(\omega, k)}{w(\omega, k)} = \frac{E\left[4k^2(k^2 - k_1^2)^{1/2}(k^2 - k_2^2)^{1/2} - (2k^2 - k_2^2)^2\right]}{2(1+\nu)k_2^2(k^2 - k_1^2)^{1/2}}, \tag{5}$$

where E is the Young's modulus, ν is the Poisson's ratio, $k_1 = \omega/c_1$, c_1 is the compressional wave speed and $k_2 = \omega/c_2$, where c_2 is the shear wave speed in the infinite medium. It would be possible to use Eq. (5) in Eq. (4) to derive a general wave equation for this geometry. This would allow a general dispersion relationship to be obtained and the behaviour of all of the possible wave types to be investigated. In this paper, we are only concerned with slow wave propagation in a thin fluid layer, and hence derive an approximate but simpler dispersion relation for this case.

For a given value of ω, the wall stiffness in Eq. (5) falls to zero for a value of k such that ω/k is equal to the speed of a Rayleigh wave. For gel-like materials, such as the tectorial membrane, with $\nu \approx 0.5$, k_2 is much larger than k_1, and the speed of a Rayleigh wave is almost the same as that of a bulk shear wave, which is equal to $(E/2(1+\nu)\rho_E)^{1/2}$ [4], where ρ_E is the density of the elastic medium. We assume, for the time being, that the fluid-elastic wave travels slowly compared with the Rayleigh wave. Under these conditions k^2 is much larger

than k_2^2 and Eq. (6) reduces to the much simpler form

$$\lim_{k^2 \gg k_2^2} \frac{p(\omega,k)}{w(\omega,k)} = \frac{kE}{(1+\nu)}, \tag{6}$$

so that in this quasi-static limit the wall stiffness is inversely proportional to the wavelength [5].

Using the relationship between $p(\omega,k)$ and $w(\omega,k)$ given by Eq. (6) in Eq. (4) gives a second-order wave equation for the fluid-elastic wave, with a wave speed of

$$c = \left[\frac{E\omega d}{(1+\nu)\rho}\right]^{1/3}, \tag{7}$$

in agreement with the corresponding result in Ref. [3]. If the density of the fluid and the elastic medium are similar, which is reasonable for the cochlear application of interest here, the assumption made above, that the wave speed in Eq. (7) is slow compared with the Rayleigh wave speed can be seen to be valid provided the thickness of the fluid layer, d, is small compared with the wavelength of the Rayleigh wave in the elastic medium, divided by 4π.

3. Application in Cochlear micromechanics

It is important to understand the micromechanical behaviour of the cochlear partition in the ear because it gives rise to the cochlear amplifier that provides us with the exquisite sensitivity and selectivity of our hearing [6,7]. A sketch of the major components of the cochlear partition is shown in Fig. 2. Previous micromechanical models, *e.g.* [8,9], have typically assumed that the basilar membrane and the tectorial membrane individually behave as single degree of freedom systems, with an associated lumped mass and stiffness. More recently, Bell and Fletcher [10] have suggested that the tectorial membrane may have a bending stiffness that acts together with the fluid inertia in the sub-tectorial gap to generate Lloyd–Redwood waves in this small space, with a wave velocity that may be slow enough that resonances can occur along the 80 μm or so length of the sub-tectorial space. Nowotny and Gummer [11] have also used a Lloyd-Redwood wave analysis to help interpret their elegant measurements of basilar membrane and tectorial membrane motion, adjacent to the sub-tectorial space. The fluid motion in this space plays an important role in coupling the inner and each of the outer hair cells, and has been included in various finite element models of the cochlea [12,13]. The first of these papers notes the development of a "complex vibrational mode" in the sub-tectorial gap. Little is known about the wave motion in this gap, but we consider here the possibility that the tectorial membrane behaves as an elastic body in such an interaction, rather than a bending plate.

There is evidence for the tectorial membrane behaving as an elastic body at audio frequencies from the results of Freeman et al. [14], who used a force probe to measure the mechanical impedance at the surface of tectorial membrane. They concluded that the dynamic behaviour up to several kilohertz could be reasonably well represented as a stiffness of about $0.2\,\mathrm{N\,m^{-1}}$ in the transverse direction, when measured with a force probe having a diameter of about 50 μm. The mechanical stiffness of an elastic half-space when measured by

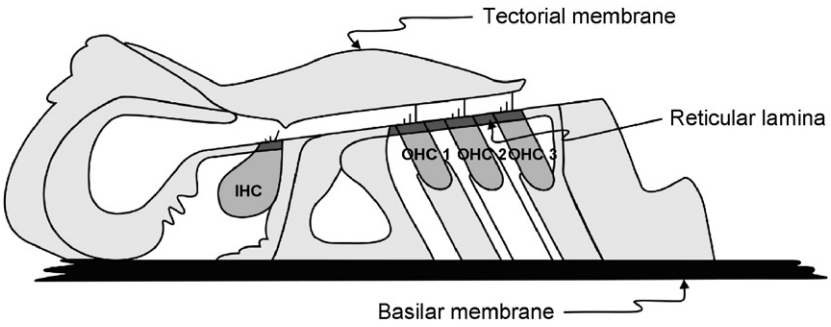

Fig. 2. The components of the organ of Corti on the basilar membrane in the cochlea, including the inner and outer hair cells (IHC and OHC).

an indenter of effective radius a is given by Shoelson et al. [15] to be approximately

$$K = \frac{Ea}{2(1-\nu)}, \tag{8}$$

where E is the Young's modulus of the elastic material and ν is its Poisson's ratio. The Young's modulus of the tectorial membrane can be estimated from this equation and the dynamic measurements of Freeman et al. [14], assuming that ν for the gel-like tectorial membrane is taken to be 0.49, as about 8 kPa, which is in reasonable agreement with the average of the static values measured by Shoelson et al. [15].

Scherer and Gummer [16] measured the mechanical impedance at various points along the upper surface of the organ of Corti, labelled the reticular lamina in Fig. 1, using an atomic force cantilever, with a typical indentation diameter of 1 μm. They also measured impedances consistent with a lossy spring, having a spring constant that fell in this case from about $0.5\,\mathrm{N\,m^{-1}}$ at the tunnel of Corti to about $0.05\,\mathrm{N\,m^{-1}}$ at the outer tunnel. Since the indenter was so much smaller in these experiments than those of Freeman et al. [14], however, the effective Young's modulus, calculated using Eq. (8), is much higher than that of the tectorial membrane, so that, to a first approximation, the reticular lamina can be assumed rigid. The large assumed difference between the Young's modulus of the tectorial membrane and that of the reticular lamina is consistent with the assumptions in the models of Cai et al. [12] and Nakajima et al. [13].

For a characteristic frequency of 1 kHz in the human cochlea, the thickness of the sub-tectorial gap, d in Section 2, is about 3 μm [17]. Assuming that the Young's modulus, Poisson's ratio and density of the tectorial membrane are 8 kPa, 0.49 and $10^3\,\mathrm{kg\,m^{-1}}$, the Rayleigh wave speed is about $1.6\,\mathrm{m\,s^{-1}}$, whereas the speed of the fluid elastic wave, given by Eq. (7) and assuming that the density of the fluid is also $10^3\,\mathrm{kg\,m^{-1}}$, is about $0.4\,\mathrm{m\,s^{-1}}$. The fluid-elastic wave is clearly slower than the Rayleigh wave, but further investigation into the effect of losses is clearly warranted in such a thin fluid layer.

4. The effect of elastic losses and fluid viscosity

For the small fluid gaps important in cochlear micromechanics the viscosity of the fluid will play a significant role in the dynamic behaviour. Measurements of the tectorial membrane dynamics also show that the stiffness has a significant loss [14]. Both of these effects will cause a propagating wave to decay and will modify the wave speed, so that it is important to take them into account. The losses measured by Freeman et al. [14] can be reasonably well modelled by assuming a complex Young's modulus for the tectorial membrane of the form:

$$E = E_o(1 + \mathrm{j}\mu), \tag{9}$$

where μ is a loss factor. This model predicts that the mechanical impedance will have a phase of $-\tan^{-1}1/\mu$. The transverse impedance measured by Freeman et al. [14] has an almost frequency-independent phase shift, of about -60° from 10 Hz to 4 kHz, so that μ is predicted to be approximately constant at audio frequencies, with a value of about 0.5.

The fluid viscosity will give rise to an additional term in the fluid momentum Eq. (3) due to drag, whose magnitude will depend on the relative values of the fluid gap thickness, d, and the viscous boundary layer thickness [18], given by

$$\delta = \left(\frac{\eta}{\rho\omega}\right)^{1/2}, \tag{10}$$

where η is the coefficient of viscosity, which is approximately $7 \times 10^{-4}\,\mathrm{kg\,m^{-1}s^{-1}}$ for cochlear fluids at body temperature. We have assumed that the tangential forces on the elastic layer due to the viscous drag can be ignored. The viscous boundary layer thickness is about 10 μm at a frequency of 1 kHz and so is somewhat larger than the fluid gap thickness, which is about 3 μm. The fluid flow in the x direction will thus have an approximately parabolic profile and the pressure gradient required to overcome viscosity will be approximately $(16\eta/d^2)\partial u/\partial t$, where u is now the average fluid displacement [18]. The fluid momentum

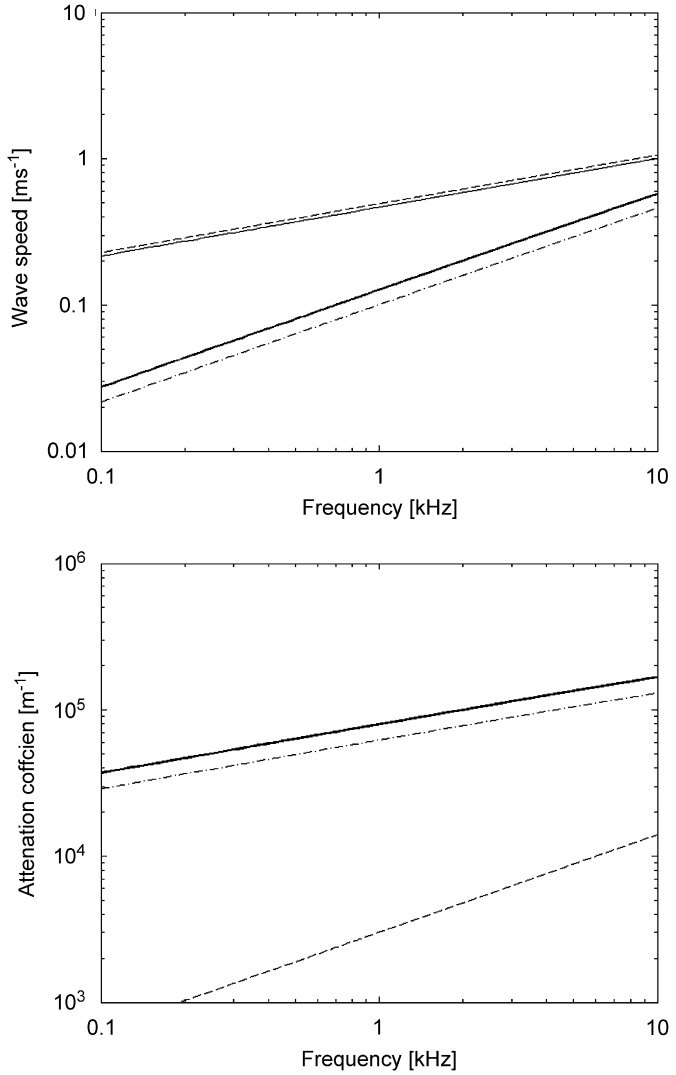

Fig. 3. The phase speed (upper) and attenuation coefficient (lower) calculated for a fluid-elastic wave in the sub-tectorial space with no losses ($\eta = 0$, $\mu = 0$), feint solid, with loss only in the elastic half space ($\eta = 0$, $\mu = 0.5$); dashed, losses in only the fluid ($\eta = 7 \times 10^{-4}$ Pas, $\mu = 0$); dot-dashed, and losses in both the elastic half space and fluid ($\eta = 7 \times 10^{-4}$ Pas, $\mu = 0.5$); thick solid.

Eq. (3), with viscosity then becomes

$$\frac{\partial p}{\partial x} = -\rho \frac{\partial^2 u}{\partial t^2} - \frac{16\eta}{d^2} \frac{\partial u}{\partial t}. \tag{11}$$

Thus Eq. (4) is modified by the effect of viscosity to become

$$-k^2 p(\omega, k) - \frac{\mathrm{j}\omega 16\eta}{d^3} w(\omega, k) + \frac{\omega^2 \rho}{d} w(\omega, k) = 0. \tag{12}$$

The relationship between $p(\omega,k)$ and $w(\omega,k)$, given by Eq. (6) in the lossless case, is now modified by the complex nature of the Young's Modulus and the wave number. Assuming that the wall stiffness is again inversely proportional to the wavelength, i.e., is proportional to the real part of k, then this relationship can be

written as

$$\frac{p(\omega,k)}{w(\omega,k)}=\frac{\mathrm{Re}[k]E_0(1+\mathrm{j}\mu)}{(1+\nu)}. \tag{13}$$

Using this in Eq. (12), the wavenumbers for the lossy case can be seen to be solutions of the equation

$$k^2\mathrm{Re}(k)=\frac{\omega^2\rho(1+\nu)}{dE_o(1+j\mu)}-\frac{\mathrm{j}16\omega\eta(1+\nu)}{d^3E_o(1+\mathrm{j}\mu)}. \tag{14}$$

Fig. 3 shows the way in which the phase speed, $\omega/\mathrm{Re}(k)$, and attenuation coefficient, $-\mathrm{Im}(k)$, calculated from Eq. (14), vary as a function of frequency if we again assume for the tectorial membrane and sub-tectorial space that $E=8\,\mathrm{kPa}$, d is $3\,\mu\mathrm{m}$, $\rho=1000\,\mathrm{kgm}^3$ and $\nu=0.49$. Four graphs are shown, for the lossless case, for loss only in the elastic half space, for loss only in the fluid, and for loss in both the elastic half space and the fluid. It can be seen that the losses in the elastic half space introduce some attenuation and a slight increase in the phase speed, whereas the fluid viscosity in this geometry leads to significant attenuation and lowers the phase speed by a factor of about three at 1 kHz, so that the wavelength is now approximately 120 μm. The overall attenuation coefficient at 1 kHz, however, is then about $10^5\,\mathrm{m}^{-1}$, so that the wave decays by a factor of $1/e$ over a length scale of about 10 μm. With this assumed geometry the fluid elastic wave is thus very heavily damped.

If the viscous term in Eq. (14) dominates the inertial one, which it does for ω much less than $16\mu/\rho d^2$, and the loss in the elastic medium is ignored, then the complex wavenumber takes the simple form

$$k=\pm(1-\mathrm{j})\left(\frac{8\omega\eta(1+\nu)}{d^3E}\right)^{1/3}. \tag{15}$$

This is analogous to the propagation of a sound wave in a capillary tube, as described by Lamb [18], except that the compliance is provided by the elastic wall here rather than the air in Lamb's case. The real and imaginary parts of the wavenumber in both cases have the same magnitude, so that the wave is attenuated by a factor of $\mathrm{e}^{-2\pi}$ (about 55 dB) every wavelength. The wave speed and attenuation coefficient predicted by Eq. (15), proportional to $\omega^{2/3}$ and $\omega^{1/3}$ respectively, fit the values calculated from Eq. (14), with μ set to zero, reasonably well up to 10 kHz, since ω is significantly less than $16\mu/\rho d^2$ in this frequency range.

5. Conclusions

It has been shown that it is possible for a fluid-elastic wave to propagate in a constrained fluid layer bounded by an elastic half-space if the thickness of the fluid layer is small compared with the wavelength of the Rayleigh wave in the elastic medium. The wave is slower than a Rayleigh wave and is dispersive, with a wavespeed proportional to $\omega^{1/3}$. The wave is further slowed if the fluid gap is small enough for viscous effects to be important, and significant attenuation is then predicted.

For parameters that seem reasonable in the mammalian cochlea, the elasticity of the tectorial membrane and the viscosity of the fluid in the sub-tectorial space are seen to interact to generate rather slow waves. These waves are very heavily damped by viscosity if the conventional theory [18] with a no slip interface condition is assumed. It has been suggested [10], however, that the effect of viscosity may be rather less significant for these biological materials, since the surfaces may be hydrophobic and the no slip condition may no longer be valid. Alternatively, the active behaviour of the outer hair cells could overcome this damping and amplify the response at certain frequencies, as observed in a model of the Lloyd-Redwood wave propagating in the sub-tectorial space [19]. An appreciation of these waves may help in understanding the results of numerical models of the cochlea and also in interpreting the direct physiological measurements within this space that are now becoming possible.

Acknowledgements

I am grateful to Professor Brian Mace for originally suggesting the wall stiffness approach and for his insightful comments, and to Dr. Ben Lineton, Dr. Emiliano Rustighi and Mr. Robert Pierzycki for interesting discussions on elasticity and cochlear mechanics. Robert Pierzycki also kindly performed the numerical simulations for the figures. I am also grateful to an anonymous reviewer for pointing out the link with the literature on geological strata and, in particular, Ref. [3].

References

[1] P. Lloyd, M. Redwood, Wave propagation in a layered plate composed of two solids with perfect contact, slip, or a fluid layer at their interface, *Acustica* 16 (1965) 224–232.
[2] W. Hassan, P.E. Nagy, On the low-frequency oscillation of a fluid layer between two elastic plates, *Journal of the Acoustic Society of America* 102 (6) (1997) 3343–3348.
[3] P.V. Krauklis, G.M. Goloshubin, L.A. Krauklis, A slow wave in a fluid layer simulating an oil-saturated seam, *Journal of Mathematical Sciences* 79 (4) (1996) 1224–1230.
[4] K.F. Graff, *Wave motion in Elastic Solids*, Dover Publications, New York (Mineola, NY), 1975.
[5] K.L. Johnson, *Contact Mechanics*, Cambridge University Press, Cambridge, 1985.
[6] J.O. Pickles, *An Introduction to the Physiology of Hearing*, Academic Press, New York (Orlando, FL/London/San Diego, CA), 1988.
[7] E. de Boer, Auditory physics. Physical principles in hearing theory. III, *Physics Reports* 208 (3) (1991) 125–231.
[8] J.B. Allen, Cochlear micromechanics—a physical model of transduction, *Journal of the Acoustic Society of America* 68 (6) (1980) 1660–1670.
[9] S.T. Neely, D.O. Kim, A model for active elements in cochlear biomechanics, *Journal of the Acoustic Society of America* 79 (5) (1986) 1472–1480.
[10] A. Bell, N.H. Fletcher, The cochlear amplifier as a standing wave: "Squirting" waves between rows of outer hair cells?, *Journal of the Acoustic Society of America* 116 (2) (2004) 1016–1024.
[11] M. Nowotny, A.W. Gummer, Nanomechanics of the subtectorial space caused by electromechanics of cochlear outer hair cells, *Proceedings of the National Academy of Science* 103 (7) (2006) 2120–2125.
[12] H. Cai, B. Shoelson, R.S. Chadwick, Evidence of tectorial membrane radial motion in a propagating mode of a complex cochler model, *PNAS* 101 (16) (2004) 62443–66248.
[13] C. Nakajima, M. Andoh, H. Wada, Finte-element analysis of the auditory transduction process in the guinea pig cochlea. *Proceedings of the 12th International Conference on Sound and Vibration (ICSV12)*, Lisbon, 2005.
[14] D.M. Freeman, C.C. Abnet, W. Hemmert, B.S. Tsai, T.F. Weiss, Dynamic material properties of the tectorial membrane: a summary, *Hearing Research* 180 (2003) 1–10.
[15] B. Shoelson, et al., Evidence and implications of inhomogeneity in Tectorial Membrane Elasticity, *Biophysical Journal* 87 (2004) 2768–2777.
[16] M.P. Scherer, A.W. Gummer, Impedance analysis of the organ of Corti with magnetically actuated probes, *Biophysical Journal* 87 (2004) 1378–1391.
[17] A. Wright, Dimensions of the cochlear stereocilia in man and the guinea pig, *Hearing Research* 13 (1984) 89–98.
[18] H. Lamb, *The Dynamical Theory of Sound*, reprinted by Dover, 1960.
[19] S.J. Elliott, R. Pierzycki, B. Lineton, Incorporation of an active feedback loop into the "squirting wave" model of the cochler amplifier, *Proceedings of the 12th International Conference on Sound and Vibration (ICSV12)*, Lisbon, 2005.